Arrangement of Orientation Pinwheel Centers around Area 17/18 Transition Zone in Cat Visual Cortex

Kenichi Ohki[1], Yoshitaka Matsuda[2], Ayako Ajima[3], Dae-Shik Kim[4] and Shigeru Tanaka

Laboratory for Neural Modeling, Brain Science Institute, RIKEN, Wako-shi, Saitama 351-01, [1]Department of Physiology, University of Tokyo School of Medicine, Hongo, Tokyo 113-0033, [2]Department of Physics, Waseda University, [3]PRESTO, JST, Japan and [4]Center for Magnetic Resonance Research, University of Minnesota Medical School, MN 55455, USA

In the primary visual cortex of higher mammals, orientation preferences are represented continuously except for singular points, so-called pinwheel centers. In spite of the uniqueness of orientation pinwheel centers, very little is known about the pattern of their arrangement. In this study we examined the arrangement of orientation pinwheel centers in the cat visual cortex by optical imaging of intrinsic signals. Our results demonstrate that orientation pinwheel centers are arranged in a unique geometric pattern around the area 17/18 transition zone: pinwheel centers of the same type are arranged in rows parallel to the transition zone, and rows of clockwise and counterclockwise pinwheel centers are arranged alternately. We suggest that the areal border imposes a strong restriction on the pattern formation of orientation preference maps in the visual cortex.

Introduction

In the mammalian visual cortex, neurons with similar response properties are clustered together, forming columns that span the entire cortical layers (Hubel and Wiesel, 1962). Along the cortical surface, visual features represented by these columns change gradually in the tangential direction. Such a systematic representation of visual features is called a 'functional map' (Hubel and Wiesel, 1963). Orientation preference is one of the most prominent visual features represented as functional maps in the primary visual cortex. The tangential layout of the orientation columns exhibits a unique feature: iso-orientation domains are arranged in a pinwheel-like fashion around singularities, referred to as 'pinwheel centers' (Braitenberg and Braitenberg, 1979; Swindale, 1982; Swindale *et al.*, 1987; Bonhoeffer and Grinvald, 1991; Blasdel, 1992). Around a pinwheel center, the preferred orientations change continuously by ± 180°, corresponding to the two types of pinwheel centers: clockwise and counterclockwise (Gotz, 1988; Blasdel, 1992).

Although relationships between pinwheel centers and other functional maps have attracted much attention in recent years (Bartfeld and Grinvald, 1992; Obermayer and Blasdel, 1993; Das and Gilbert, 1997; Crair *et al.*, 1997a,b; Hubener *et al.*, 1997), there have been very few reports on their arrangement *per se*, except some studies reporting no evidence for geometric patterns of pinwheel centers in area 17 proper (Obermayer and Blasdel, 1997). Since theoretical studies have suggested that the areal border has a boundary effect on the pattern formation of functional maps (Swindale, 1980; Lowel and Singer, 1990; Wolf *et al.*, 1996), some regular structure in the arrangement of pinwheel centers might be expected around the areal border.

Cytoarchitectonically, the area 17/18 border in the cat visual cortex is not a sharp border but a 1- to 1.5-mm-wide transition zone (Otsuka and Hassler, 1962; Payne, 1990). The transition zone represents a strip of the ipsilateral visual field (Payne, 1990) and is connected to retinotopically corresponding locations in the areas 17 and 18 in the opposite hemisphere via non-mirror-symmetric callosal connections (Payne, 1991; Payne and Siwek, 1991; Olavarria, 1996). Previous studies about functional organization of the transition zone have examined continuity (Orban *et al.*, 1980; Lowel and Singer, 1987; Lowel *et al.*, 1987; Diao *et al.*, 1990; Bonhoeffer *et al.*, 1995) and orthogonality (Lowel and Singer, 1987; Lowel *et al.*, 1987; Diao *et al.*, 1990) of functional maps to the transition zone, while the arrangement of pinwheel centers has not been examined yet around the transition zone with discriminating types of pinwheel centers.

In this study, we focused on examining the arrangement of pinwheel centers across the area 17/18 transition zone. To examine the detailed arrangement, we used optical imaging of intrinsic signals because of its high spatial resolution. Our results demonstrate for the first time that the orientation pinwheel centers are arranged to form a unique geometric pattern around the area 17/18 transition zone in the cat visual cortex.

Materials and Methods

Young cats (n = 8, 2–3 months old, 500–1200 g) were initially anesthetized with ketamine (15 mg/kg, A.m.) and xylazine (2.5 mg/kg, A.m.). A tracheotomy was performed and the animals were artificially ventilated with a 1:1 mixture of N_2O/O_2 containing 0.5–1.0% isoflurane. The electrocardiogram, end-tidal CO_2, arterial oxygen saturation and rectal temperature were continuously monitored and maintained within normal limits throughout the experiment. The animals were paralyzed with pancuronium bromide (0.1 mg/kg/h, A.v.). A craniotomy was performed with its center around the Horsley–Clark 0 to expose the area 17/18 transition zone in the lateral gyrus in cats A, B and C, around P9–L6 to expose the area 17/18 transition zone in the postlateral gyrus in cat D and around P5 to expose both the area 17/18 transition zone in the lateral gyrus and the inside of area 17 which was >1 mm away from the transition zone in cats E, F, G and H. In cats F, G and H, the area 17/18 transition zone was revealed in a small portion, and only data from area 17 proper were analyzed. A stainless steel chamber was cemented onto the skull. After removal of the dura, the chamber was filled with silicon oil and sealed with a coverglass. The eyes were focused on a monitor using appropriate contact lenses. The animals were cared for in accordance with the 'Guiding Principles for the Care and Use of Animals in the Field of Physiological Science' of the Japanese Physiological Society and 'NIH Guide for the Care and Use of Laboratory Animals'.

Optical Imaging

Intrinsic optical signals were measured to visualize functional maps across the area 17/18 transition zone using standard techniques (Bonhoeffer and Grinvald, 1996). The cortex was illuminated with a 630 nm light and the focal plane was adjusted at 400–600 μm below the cortical surface using a tandem-lens macroscope arrangement (Ratzlaff and Grinvald, 1991). Images were obtained with a CCD video camera (648 × 480 pixels) and digitized by a differential video-enhancement system, Imager 2001 (Optical Imaging, Germantown, NY).

The animals were stimulated with full-screen, high-contrast, moving square-wave gratings displayed on a 20 inch CRT monitor positioned 30 cm in front of the animal. The gratings consisted of two spatial frequencies (0.15 and 0.5 cycles/degree), six orientations separated by 30° and both directions of motion. The temporal frequency was

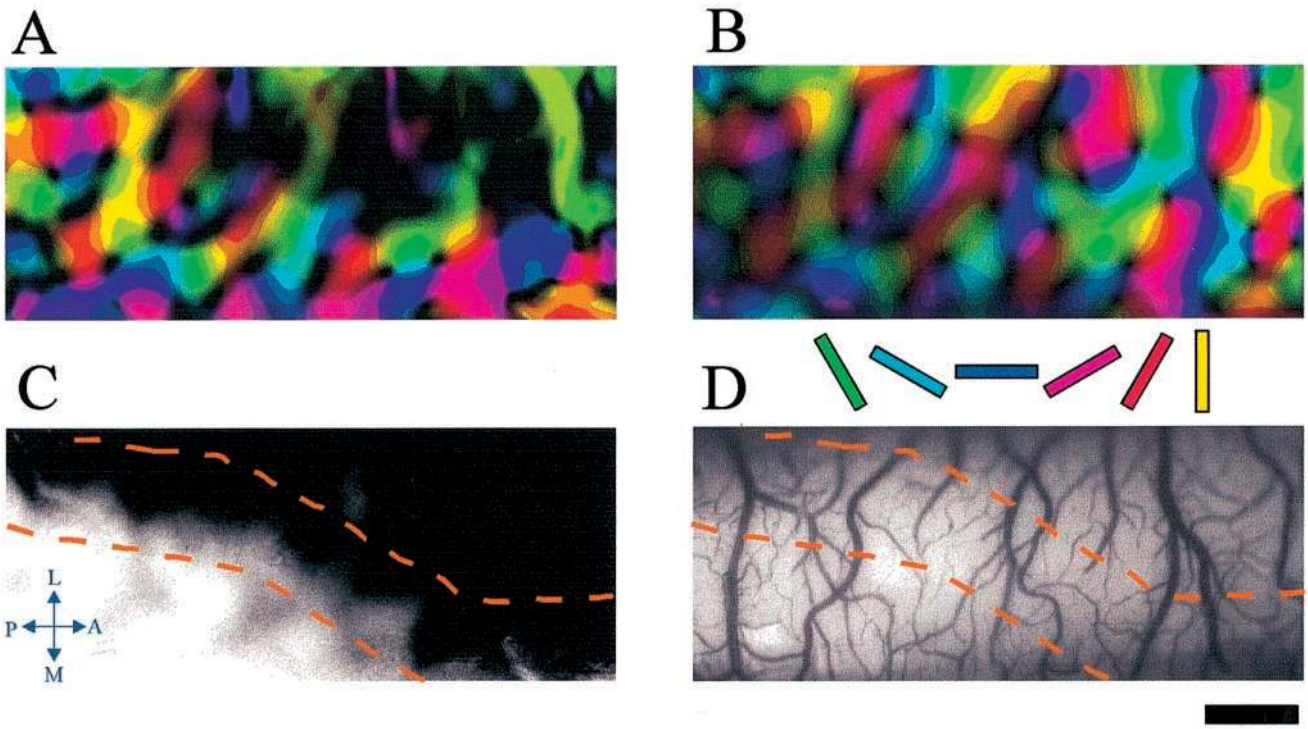

Figure 1. Definition of the area 17/18 transition zone. (*A*) An orientation preference polar map obtained with gratings of a high spatial frequency (0.5 cycle/degree, 2 Hz). The angle of the preferred orientation is coded by the hue of the color according to the key shown at the bottom of (*B*). The magnitude of the orientation-selective response is coded by the brightness of the color. (*B*) An orientation preference polar map obtained with gratings of a low spatial frequency (0.15 cycle/degree, 2 Hz). (*C*) Spatial frequency preference map. The sum of the responses to low spatial frequency stimuli over all orientations is divided by the sum of responses to high spatial frequency stimuli at each pixel of the recorded region. The black and white regions indicate preference for low and high spatial frequency stimuli, respectively. Location of the area 17/18 transition zone is defined as the 1-mm-wide zone delineated by the two dashed lines. A, anterior; P, posterior; M, medial; L, lateral. (*D*) Cortical blood vessel pattern in the imaged region. Scale bar, 1 mm.

maintained at 2.0 Hz. The responses to each stimulus were summed between 1.0 and 5.0 s after the onset of stimulus movement, while the stimulus was presented 64–160 times in a pseudo-random sequence.

Data Analysis

Data analysis was performed using IDL (Research Systems Inc., Boulder, CO). To obtain a 'single-condition map', the cortical image obtained for one stimulus was divided by the 'cocktail blank', the sum of the images obtained for all stimuli and band-pass filtered with a Gaussian kernel of 70–1000 μm radius. Then all the single-condition maps in response to the six orientations of the gratings were summed vectorially, pixel by pixel. The angle of the resultant vector corresponds to the preferred orientation and the length of the vector ('magnitude') corresponds to the orientation-specific signal strength of that pixel. The 'angle map' shows only the preferred orientation, by means of color-coding. The 'polar map' shows the preferred orientation as the hue of the color, and the magnitude as the brightness of the color. The positions of the orientation pinwheel centers were detected automatically and checked visually as the points at which the integral of the orientation differences around a pixel was ± 180° (Crair *et al.*, 1997a). The integral paths were always taken in a counterclockwise direction. The point was defined as a counterclockwise pinwheel center when the integral was +180°, and as a clockwise pinwheel center when the integral was –180°. The stability of pinwheel centers was confirmed by using several different band-pass filters.

Delineation of the Area 17/18 Transition Zone

Based on the property that neurons in area 18 prefer visual stimuli with spatial frequencies that are, on average, one-third as high as those preferred by area 17 neurons (Movshon *et al.*, 1978), the functional area 17/18 transition zone can be visualized *in vivo* (Bonhoeffer *et al.*, 1995). Figure 1*a* shows a polar map obtained with gratings of a high spatial frequency (0.5 cycles/degree, 2 Hz). The activated region was limited to the posteromedial part of the image, which corresponds to area 17. Figure 1*b* shows a polar map on the same cortical surface in response to gratings of a low spatial frequency (0.15 cycles/degree, 2 Hz). Although the whole imaged area was activated, the anterolateral part, which corresponds to area 18, showed stronger response than the posteromedial part. Figure 1*c* shows a map depicting the ratio of the response strength recorded with the low spatial frequency stimuli (optimal for area 18) to the response strength recorded with the high spatial frequency stimuli (optimal for area 17). The white and black regions indicate preference to the area 17-optimal and area 18-optimal stimuli, respectively. The spatial frequency preference changes smoothly and rapidly at the ~1-mm-wide narrow band-like gray region between the white and black regions (Bonhoeffer *et al.*, 1995). We delineated this spatial frequency preference transition zone as where the spatial frequency preference changes rapidly. Briefly, the steepness of the change of spatial frequency preference was defined as the length of the gradient vector of the spatial frequency map after smoothing. The region of high steepness was defined as the spatial frequency transition zone. Because the spatial frequency preference transition zone is known to correlate well with the anatomical area 17/18 transition zone (Orban *et al.*, 1980; Sheth *et al.*, 1996), we regarded this region as the area 17/18 transition zone. The transition zone defined from the spatial frequency preferences always ran from the anteromedial to the posterolateral part in the lateral gyrus in all the cats examined, which is consistent with the anatomical and retinotopical area 17/18 transition zone (Otsuka and Hassler, 1962; Tusa *et al.*, 1978).

We also confirmed by optical imaging that the transition zone of spatial frequency preference coincides with the retinotopical area 17/18 transition zone defined as the representation of the ipsilateral visual field (Payne, 1990) (Fig. 2). After the spatial frequency preference map was obtained (Fig. 2*A*) in the same manner as in Figure 1*c*, the animal was paralyzed with gallamine triethiodide (10 mg/kg/h, A.v.) to minimize eye

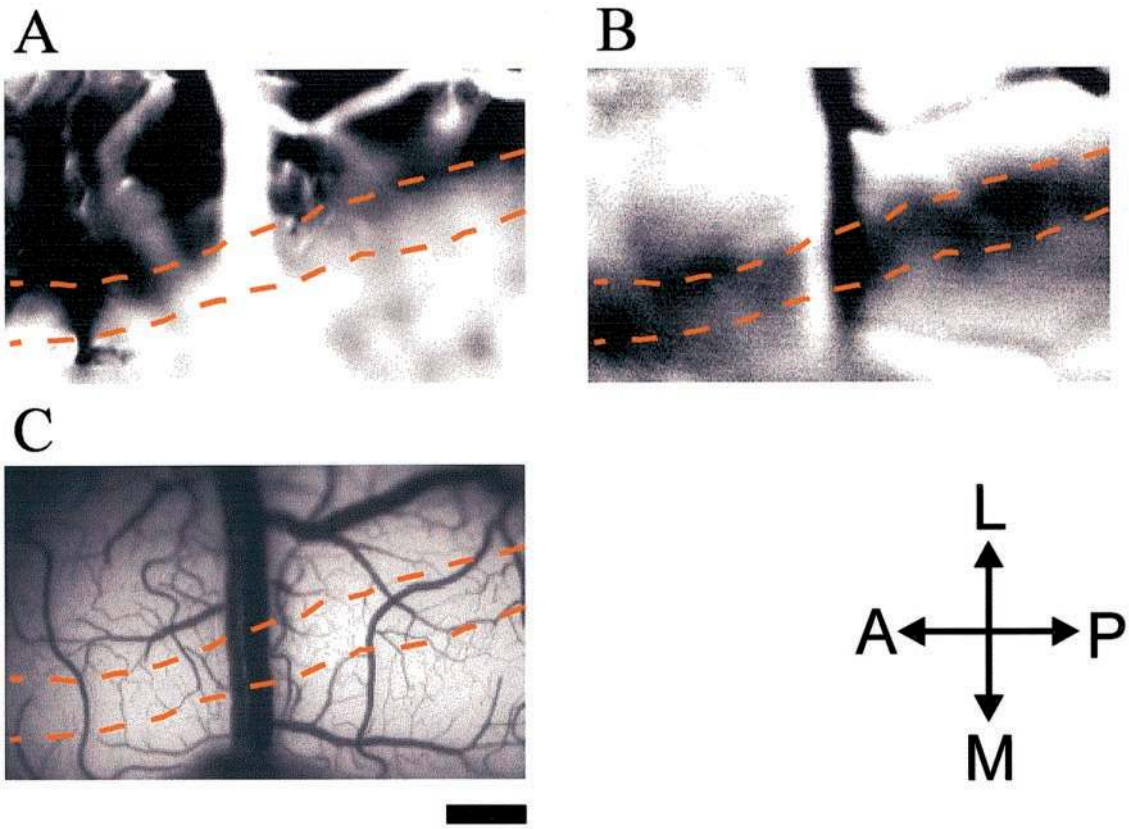

Figure 2. Coincidence of the spatial frequency preference transition zone with the retinotopical area 17/18 transition zone. (*A*) Spatial frequency preference map. The sum of responses to low spatial frequency (0.15 cycle/degree) gratings is divided by the sum of responses to high frequency (0.5 cycle/degree) gratings. The black and white indicate preference for low and high spatial frequency stimuli, and correspond to areas 18 and 17, respectively. The orange dashed lines show the transition zone of the spatial frequency preference. (*B*) Representation of the ipsilateral visual field in the area 17/18 transition zone. The sum of responses to gratings presented in the ipsilateral visual field is divided by the sum of responses to gratings in the contralateral visual field. The black diagonal band-like region corresponds to the representation of the ipsilateral visual field and can be regarded as the retinotopically defined area 17/18 transition zone. The orange dashed lines show the transition zone of the spatial frequency preference defined in (*A*). (*C*) Cortical blood vessel pattern of the imaged region. A, anterior; P, posterior; M, medial; L, lateral. Scale bar, 1 mm.

movement and the ipsilateral eye was closed. The position of the opened contralateral eye was checked every hour and its stability was confirmed. The stimuli were consisted of moving grating of four orientations with low spatial frequency (0.15 cycles/degree) and were confined to either the contralateral or the ipsilateral side. The position of the border between the ipsilateral and the contralateral side was changed systematically with a step of 1°, over 10–18° ipsilateral from the center of the optic disk of the contralateral eye. When the position came to the 15° ipsilateral from the optic disk, the representation of the ipsilateral side was clearly confined in an ~1-mm-wide narrow band-like region (Fig. 2*B*), and this region was regarded as the retinotopical area 17/18 transition zone. The orange dashed lines in Figure 2*A*,*B* show the transition zone of spatial frequency preference defined in Figure 2*A* and precisely coincides with the retinotopical transition zone in Figure 2*B*.

Simulation

In order to understand the possible mechanism of arrangement of pinwheel centers, we conducted simulation study. To construct orientation preference maps, we selected bandpass filter model (Rojer and Schwarz, 1990) because of its simplicity and one of its properties: the nearest neighbor pinwheel centers tend to be of opposite types, that is, clockwise and counterclockwise (Obermayer and Blasdel, 1997; Tal and Schwartz, 1997). To overcome an unrealistic property (Erwin *et al.*, 1995) in orientation preference maps produced by this method, we modified it in the following way. We first prepared a pair of two-dimensional white noises which were both convoluted with two-dimensional bandpass filter repeatedly (typically 20 times). A pair of the yielded two-dimensional patterns were regarded as a pair of single condition maps which represent 0°/90° and 45°/135°. An orientation preference map was then calculated as the pixel-by-pixel vectorial summation of two maps in the same manner as described in Data Analysis.

In this model, near-excitatory far-inhibitory lateral interaction is assumed and it is represented as a band-pass filter (Rojer and Schwarz, 1990):

$$F(x,y) = (1/2\pi\sigma_{Ex}\sigma_{Ey})\exp(-x^2/2\sigma_{Ex}^2 - y^2/2\sigma_{Ey}^2) - (1/2\pi\sigma_{Ix}\sigma_{Iy})\exp(-x^2/2\sigma_{Ix}^2 - y^2/2\sigma_{Iy}^2)$$

We assumed the direction of the areal border to be horizontal. To realize the orthogonality between iso-orientation contours and the areal border, we assumed anisotropy in the lateral interaction (Swindale, 1980; Rojer and Schwartz, 1990). This is the only way to introduce orthogonality in this model. It seems reasonable also from the experimental observations as follows: in both models, the autocorrelation function of the orientation preference map takes a shape similar to the lateral interactions. Autocorrelation functions of orientation maps around the area 17/18 transition zone obtained from experiments show anisotropy with the long axis orthogonal to the direction of the transition zone. Therefore, the lateral interaction is also expected to have anisotropy.

We used three kinds of anisotropy: (A) only far-inhibitory interaction is elongated parallel to the border (σ_{Ex} = 140, σ_{Ey} = 140, σ_{Ix} = 310, σ_{Iy} = 288 μm); (B) both near-excitatory and far-inhibitory interactions are elongated orthogonal to the border (σ_{Ex} = 112, σ_{Ey} = 224, σ_{Ix} = 230, σ_{Iy} = 460 μm); and (C) only near-excitatory interaction is elongated orthogonal

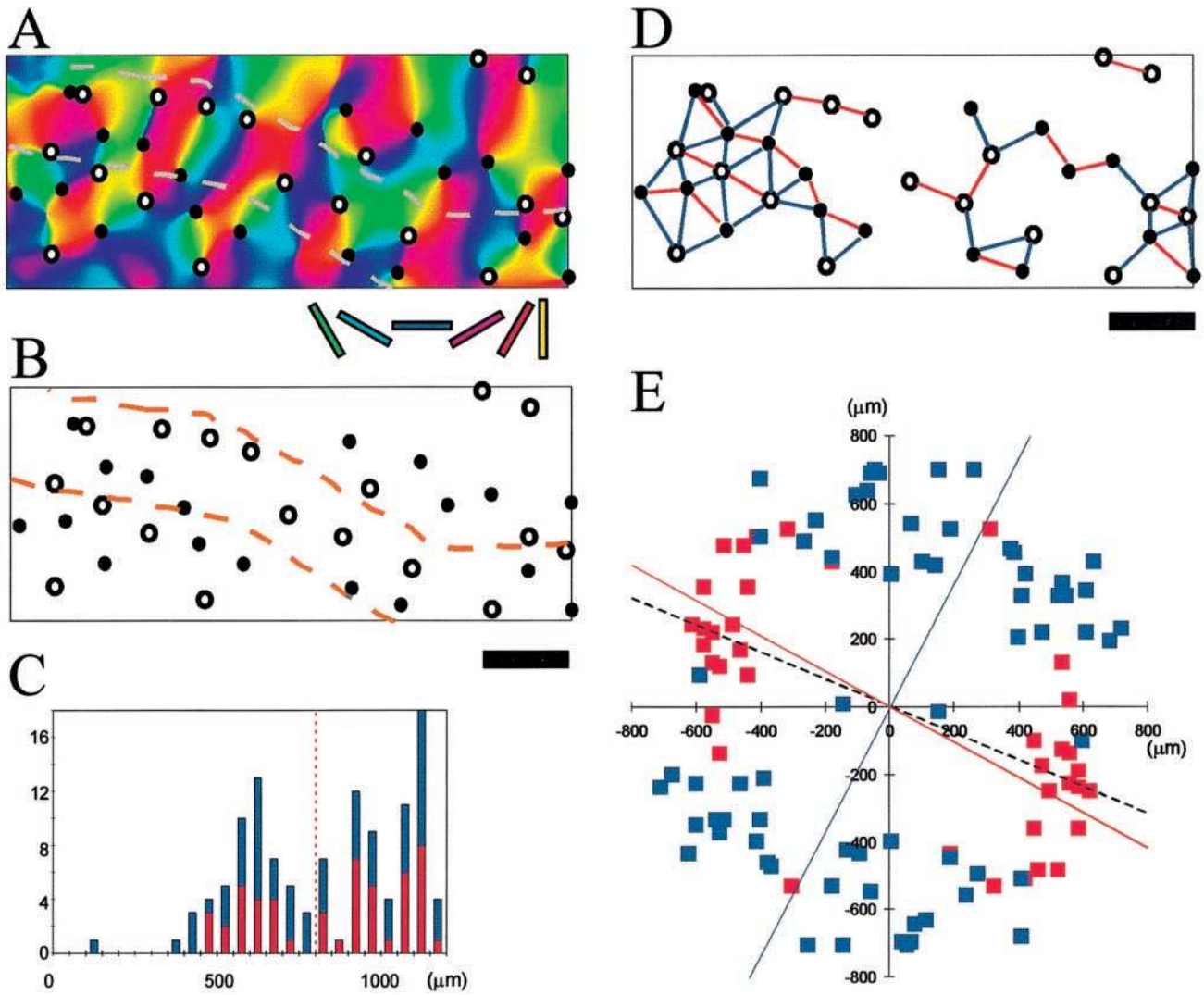

Figure 3. Arrangement of orientation pinwheel centers around the area 17/18 transition zone. (*A*) Orientation preference map and orientation pinwheel centers in the same animal as in Figure 1. Filled and open circles represent clockwise and counterclockwise pinwheel centers. Dashed lines show the location of the area 17/18 transition zone. Only the pinwheel centers and the area 17/18 transition zone are depicted again in (*B*). (*C*) Distribution of distances among all the pairs of pinwheel centers in (*B*). Red and blue bars indicate the number of pinwheel pairs of the same type and opposite types, respectively. (*D*) Definition of neighboring pairs of pinwheel centers. When two pinwheel centers are located within a distance of 800 μm from each other (red dashed line in *C*), they are defined as neighboring pinwheel centers. Red and blue line segments connect pairs of neighboring pinwheel centers of the same type and opposite types, respectively. There are 19 pairs of the same type and 29 pairs of opposite types. (*E*) A scattergram of the relative positions of neighboring pinwheel centers. Since a line segment in (*D*) was counted twice to construct this plot, two points located at opposite sides with respect to the origin correspond to a single line segment in (*D*). Because of it, just half of the data points in (*E*) were used in the later statistical analyses. The abscissa and ordinate show the distance between neighboring pinwheel centers along the anterior–posterior and lateral–medial axes, respectively. The red and blue squares represent the pinwheel pairs of the same type and opposite types, respectively. The red and blue solid lines indicate the directions of the first principal components for the pairs of the same type and opposite types, respectively. The dashed line represents the average direction of the area 17/18 transition zone.

to the border (σ_{Ex} = 140, σ_{Ey} = 150, σ_{Ix} = 310, σ_{Iy} = 310 μm). The shapes of these interactions are illustrated in the top part of Figure 5. With these parameters, the measured degree of orthogonality was obtained (Fig. 5*D*). In the experiments, percentage of opposite-type in the nearest-neighbor pinwheel centers was 69.9 ± 9.1% (n = 5; cats A–E; mean ± SD). To incorporate this statistic, simulated results outside of a range of 69.9 ± 9.1% were discarded.

We also conducted simulations with isotropic interaction to model the orientation preference map in the area 17 proper, because the orientation map in the area 17 was nearly isotropic consistently in our observations. Almost all simulations (97.5%) resulted in no significant tendency in the distribution of pinwheel centers. This is compatible with no systematic arrangement of orientation pinwheel centers observed in the area 17 proper (cats E′, F, G and H).

Results

As a first step, we delineated the transition zone between areas 17 and 18 by optical imaging (Fig. 1) according to the procedure described in Materials and Methods.

Arrangement of Orientation Pinwheel Centers

To examine the arrangement of orientation pinwheel centers, the positions of clockwise and counterclockwise pinwheel centers in the same animal as in Figure 1 were detected using the algorithm described in Materials and Methods (Fig. 3*A*,*B*). Visual inspection of Figure 3*B* reveals that the pinwheel centers are arranged in a unique geometric pattern relative to the area 17/18 transition zone: both the clockwise pinwheel centers (filled

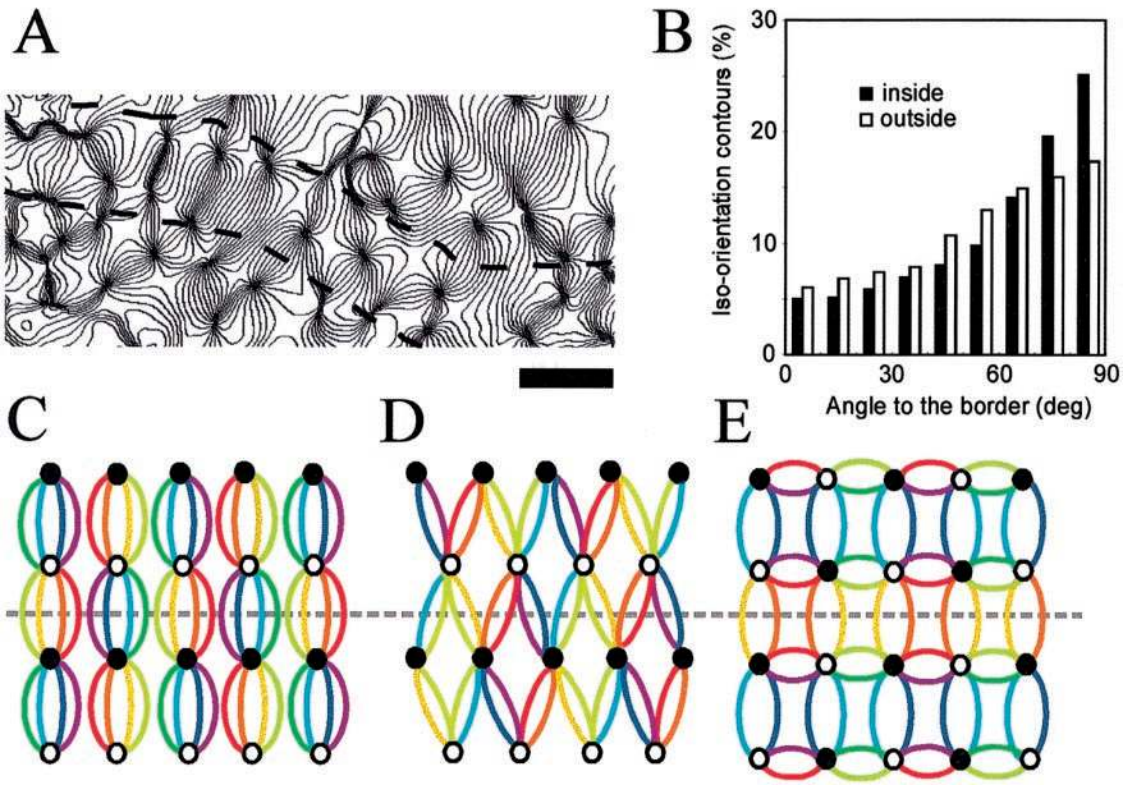

Figure 4. Orthogonal relationship between the iso-orientation contours and the area 17/18 transition zone. (*A*) Iso-orientation contour map. Each solid line represents an iso-orientation contour. The dashed lines delineate the area 17/18 transition zone. Scale bar, 1 mm. (*B*) Histograms of relative angles between the iso-orientation contours and the average direction of the area 17/18 transition zone. The histograms were obtained by counting pixels at which the iso-orientation contour runs at a particular angle in the abscissa to the average direction of the transition zone, and plotted separately for inside (filled bars) and outside (open bars) the transition zone. (*C–E*) Schemata of arrangements of the pinwheel centers. (*C*) Idealized arrangement of pinwheel centers, where pinwheel pairs of the same type are arranged parallel to the border, and pinwheel pairs of opposite types are located orthogonal to the border. Each colored curve represents an iso-orientation contour and the color indicates the preferred orientation. The black and white dots represent clockwise and counterclockwise pinwheel centers. The gray dashed line represents the direction of the areal border. (*D*) Another arrangement of pinwheel centers which is also compatible with the global arrangement observed in this study. In this case, pinwheel pairs of opposite types are not arranged orthogonal to the areal border. (*E*) An unlikely arrangement of pinwheel centers in which some iso-orientation contours run parallel to the border.

circles) and the counterclockwise pinwheel centers (open circles) are aligned parallel to the transition zone. The rows composed of clockwise pinwheel centers and those composed of counterclockwise pinwheel centers are arranged alternately, in the direction orthogonal to the border. Similar patterns of orientation pinwheel centers were also observed in all the other animals.

Quantitative Evaluation

To confirm objectively the results of visual inspection, we evaluated the local arrangement of pinwheel centers quantitatively using principal components analysis.

Initially, to define neighboring pinwheel centers, we used the distribution of distances among all the pairs of pinwheel centers as shown in Figure 3*C*. The first peak appearing at ~600 μm showed unimodal distribution up to 800 μm. Therefore, when two pinwheel centers were located within a distance of 800 μm from each other, they were defined as neighboring pinwheel centers. Pairs of neighboring pinwheel centers are displayed as line segments in Figure 3*D*.

Secondly, the relative positions from any pinwheel centers to their neighboring pinwheel centers are plotted in Figure 3*E*. Red squares, representing pinwheel pairs of the same type, and blue squares, representing pinwheel pairs of opposite types, are separately clustered. Finally, we applied the principal component analysis to the scattergram of the red and blue squares, respectively. The axis of the first principal component (θ_{1stPC}) indicates the direction of the clustering of the data points, and the ratio of the first principal component eigenvalue to the second one ($\sigma1/\sigma2$) reflects the strength of clustering. Pairs of the same type are strongly clustered around the red line, as shown in Figure 3*E*, which nearly coincides with the average direction of the area 17/18 transition zone ($|\theta_{1stPC} - \theta_{TZ}|$ (same type) = 6°). On the other hand, pairs of opposite types are weakly clustered around the blue line, which is approximately orthogonal to the transition zone ($|\theta_{1stPC} - \theta_{TZ}|$ (opposite type) = 85°). The eigenvalue ratio is 5.59 for pairs of the same type [$\sigma1/\sigma2$ (same type) = 5.59] and 2.02 for pairs of opposite types [$\sigma1/\sigma2$ (opposite type) = 2.02], suggesting that the clustering is stronger for the pairs of the same type. These clusterings indicate that pairs of the same type have a strong tendency to be located parallel to the transition zone, while pairs of opposite types have a weak tendency to be located orthogonal to the transition zone. The observed global arrangement in Figure 3*B* was, therefore, confirmed objectively by this local arrangement of pinwheel centers (Fig. 4*C*). Principal component analysis was also applied to arrangements of pinwheel centers in the other animals and they showed the same tendency (Table 1).

Statistical Evaluation

To see the statistical significance of the local arrangement of pinwheel centers as revealed by the principal component

Table 1
Summary of statistics of pinwheel center arrangement

	cat A	cat B	cat C	cat D	cat E	cat E′	cat F	cat G	cat H
Recording area	TZ	TZ	TZ	TZ	TZ	17	17	17	17
$\lvert\theta_{1stPC} - \theta_{TZ}\rvert$ (same type) (deg)	6	3	1	13	12	30	85	15	11
$\lvert\theta_{1stPC} - \theta_{TZ}\rvert$ (opposite type) (deg)	85	85	88	58	65	13	26	25	4
$\sigma1/\sigma2$ (same type)	5.59	6.85	7.49	15.07	4.71	1.10	1.76	2.36	1.64
$\sigma1/\sigma2$ (opposite type)	2.02	2.63	2.62	1.87	1.82	1.24	1.36	1.17	1.14
$\lvert\theta_{same} - \theta_{TZ}\rvert < 45$ deg	$P < 5 \times 10^{-5}$	$P < 2 \times 10^{-5}$	$P < 2 \times 10^{-4}$	$P < 1 \times 10^{-4}$	$P < 0.002$	n.s.	n.s.	n.s.	n.s.
$\lvert\theta_{opposite} - \theta_{TZ}\rvert > 45$ deg	$P < 0.002$	n.s.	$P < 0.05$	n.s.	n.s.	n.s.	n.s.	n.s.	n.s.
$\lvert\theta_{same} - \theta_{TZ}\rvert < \lvert\theta_{opposite} - \theta_{TZ}\rvert$	$P < 2 \times 10^{-7}$	$P < 0.005$	$P < 1 \times 10^{-5}$	$P < 5 \times 10^{-6}$	$P < 0.02$	n.s.	n.s.	n.s.	n.s.

TZ, area 17/18 transition zone; 17, area 17 proper; θ_{1stPC}, direction of the first principal component; θ_{TZ}, average direction of the area 17/18 transition zone; $\sigma1$, $\sigma2$, eigenvalues of the first and second principal components; n.s., not significant ($P > 0.05$); θ_{same}, $\theta_{opposite}$, directions of the line segments connecting pinwheel pairs of the same type and opposite types.

analysis, we examined the distribution of angles between the line segments linking pairs of neighboring pinwheel centers (Fig. 3*D*) and the average direction of the area 17/18 transition zone. The average value of the angles between the line segments linking pairs of the same type and the direction of transition zone ($|\theta_{same} - \theta_{TZ}|$) was 19°, and significantly smaller than 45° ($|\theta_{same} - \theta_{TZ}| < 45°$; $P < 5 \times 10^{-5}$; two-tailed Student's *t*-test), indicating that pinwheel pairs of the same type were likely to be aligned parallel to the direction of the transition zone. On the other hand, the average value of the angles between the line segments linking pinwheel pairs of opposite types and the direction of transition zone ($|\theta_{opposite} - \theta_{TZ}|$) was 57°, and significantly larger than 45° ($|\theta_{opposite} - \theta_{TZ}| > 45°$; $P < 0.002$; two-tailed Student's *t*-test), indicating that pairs of opposite types were likely to be aligned orthogonal to the transition zone. The difference between these two angles was significant ($|\theta_{same} - \theta_{TZ}| < |\theta_{opposite} - \theta_{TZ}|$; $P < 2 \times 10^{-7}$; two-tailed Welch's *t*-test). The results of statistical analyses in the five animals are summarized in Table 1. In all the animals examined in this study, the tendency of pinwheel pairs of the same type to be aligned parallel to the area 17/18 transition zone was statistically significant. This result confirms the existence of similar global arrangements in these animals.To see the statistical significance of the local arrangement of pinwheel centers as revealed by the principal component analysis, we examined the distribution of angles between the line segments linking pairs of neighboring pinwheel centers (Fig. 3*D*) and the average direction of the area 17/18 transition zone. The average value of the angles between the line segments linking pairs of the same type and the direction of transition zone ($|\theta_{same} - \theta_{TZ}|$) was 19°, and significantly smaller than 45° ($|\theta_{same} - \theta_{TZ}| < 45°$; $P < 5 \times 10^{-5}$; two-tailed Student's *t*-test), indicating that pinwheel pairs of the same type were likely to be aligned parallel to the direction of the transition zone. On the other hand, the average value of the angles between the line segments linking pinwheel pairs of opposite types and the direction of transition zone ($|\theta_{opposite} - \theta_{TZ}|$) was 57°, and significantly larger than 45° ($|\theta_{opposite} - \theta_{TZ}| > 45°$; $P < 0.002$; two-tailed Student's *t*-test), indicating that pairs of opposite types were likely to be aligned orthogonal to the transition zone. The difference between these two angles was significant ($|\theta_{same} - \theta_{TZ}| < |\theta_{opposite} - \theta_{TZ}|$; $P < 2 \times 10^{-7}$; two-tailed Welch's *t*-test). The results of statistical analyses in the five animals are summarized in Table 1. In all the animals examined in this study, the tendency of pinwheel pairs of the same type to be aligned parallel to the area 17/18 transition zone was statistically significant. This result confirms the existence of similar global arrangements in these animals.

In one animal, we recorded orientation maps around the 17/18 transition zone and inside area 17 simultaneously (cat E in Table 1). A similar systematic arrangement of pinwheel centers was observed around the area 17/18 transition zone but not inside area 17 which is >1 mm away from the transition zone. In the last animal, we recorded orientation maps inside area 17, and systematic arrangement was also not observed (cats F, G and H in Table 1). In one animal, we recorded orientation maps around the 17/18 transition zone and inside area 17 simultaneously (cat E in Table 1). A similar systematic arrangement of pinwheel centers was observed around the area 17/18 transition zone but not inside area 17 which is >1 mm away from the transition zone. In the last animal, we recorded orientation maps inside area 17, and systematic arrangement was also not observed (cats F, G and H in Table 1).

Orthogonality

Finally, we confirmed previous findings about the area 17/18 transition zone. It has been reported that orientation columns in cat visual cortex tend to run across the transition zone at right angles (Lowel *et al.*, 1987; Diao *et al.*, 1990). Similarly, in our study, the orthogonality between the iso-orientation contours and the direction of area 17/18 transition zone was observed clearly within the transition zone, and weakly even outside the transition zone (Fig. 4*A*,*B*).

Discussion

In this study, we found a characteristic arrangement of orientation pinwheel centers around the area 17/18 transition zone. Globally, pinwheel centers of the same type were arranged in rows parallel to the area 17/18 transition zone, and alternating rows of the clockwise and counterclockwise pinwheel centers were arranged in the direction orthogonal to the transition zone. This global arrangement is similar to the configurations of pinwheel centers in Figure 4*C*,*D*. Pinwheel pairs of the same type are arranged parallel to the areal border in both Figure 4*C* and Figure 4*D*, while pinwheel pairs of opposite types are arranged orthogonal to the areal border in Figure 4*C* but not in Figure 4*D*. These tendencies can be seen in Table 1: the tendency of pinwheel pairs of the same type to be arranged parallel to the transition zone was statistically significant in all the animals, while the tendency of pinwheel pairs of opposite types to be arranged orthogonal to the transition zone was not always statistically significant.

Relationship to Other Features of Pinwheel Centers

Since the finding of orientation pinwheel centers (Bonhoeffer and Grinvald, 1991), two issues have been clarified about their arrangement, namely (i) pinwheel centers tend to be located in the middle of ocular dominance columns (Bartfeld and Grinvald, 1992; Obermayer and Blasdel, 1993; Crair *et al.*, 1997a; Hubener

et al., 1997) and (ii) the nearest neighbor pinwheel centers tend to be of opposite types (Obermayer and Blasdel, 1997; Tal and Schwartz, 1997). Although the former might be thought to influence the positions of pinwheel centers, it does not impose any restrictions on the types of pinwheel centers. When the types of pinwheel centers in Figure 3*B* were randomly assigned, the probability of obtaining some systematic arrangement was extremely low (<3% in Monte Carlo simulation). The latter property does not restrict pairs of pinwheel centers in specific directions and will not cause pinwheel pairs of the same type to be aligned parallel to the transition zone. Therefore, it is difficult to explain our finding based only on two known properties of orientation pinwheel centers, both of which are not specific to the border region but are also valid in the area 17 proper. We speculate that some property specific to the border region contributes to the systematic arrangement of pinwheel centers.

Boundary Effect on Pattern Formation

For the organization of functional maps in the cerebral cortex, the importance of activity-dependent refinement of neuronal connections has been pointed out (Wiesel and Hubel, 1965; Hubel *et al.*, 1977; Stryker and Strickland, 1984; Stryker and Harris, 1986; Shatz, 1990; Weliky and Katz, 1997; Crair *et al.*, 1998; Sengpiel *et al.*, 1999). It has also been considered theoretically that these functional maps are self-organized in an activity-dependent manner during development (Linsker, 1986; Tanaka, 1990; Miller, 1994). In self-organizing pattern formation, boundary conditions play an essential role in determining the final pattern. Therefore, in the visual cortex, the boundary condition imposed by the areal border is expected to be one of the important constraints on the layout of orientation columns (Wolf *et al.*, 1996). The close relationship between the arrangement of pinwheel centers and the direction of the transition zone in our study supports the idea that the arrangement of pinwheel centers is a consequence of the boundary effect of the area 17/18 transition zone on the pattern formation of orientation maps.

Relationship to Orthogonality

One of characteristic features of functional maps often observed around the areal border is a tendency for columns to run perpendicular to the border. In the primate striate cortex, ocular dominance columns run perpendicular to the V1/V2 border (LeVay *et al.*, 1975), as do the thick, thin and pale stripes in primate V2 (Livingstone and Hubel, 1982; Tootell *et al.*, 1983) and the orientation columns in the tree shrew striate cortex (Humphrey *et al.*, 1980; Bosking *et al.*, 1997). In areas 17 and 18 in cats (Lowel and Singer, 1987; Lowel *et al.*, 1987; Diao *et al.*, 1990) and ferrets (Law *et al.*, 1988; Chapman *et al.*, 1996), both the orientation and ocular dominance columns tend to intersect the area 17/18 border at right angles. Such orthogonality of stripe patterns to the boundary is a general feature of a self-organizing pattern formation (Greenside *et al.*, 1982) and it has been proposed that these orthogonalities are due to the boundary effect imposed by the areal border (Swindale, 1980; Lowel and Singer, 1990).

Our results also indicated that iso-orientation contours tend to run orthogonal to the area 17/18 transition zone (Fig. 4*A*,*B*). Since iso-orientation contours link adjacent pairs of clockwise and counterclockwise pinwheel centers (Obermayer and Blasdel, 1993), there might be a mutual constraint between the direction of iso-orientation contours and the arrangement of pinwheel centers. We examined whether the arrangement of pinwheel centers observed in our study is related to the orthogonality of the iso-orientation contours to the transition zone. As described in Results, the orthogonality is observed both inside and outside the transition zone. To satisfy the orthogonality in the wide areas, the configurations shown in Figure 4*C*,*D*, which are similar to our observations, would be preferable to that shown in Figure 4*E*, in which some iso-orientation contours run parallel to the border around the transition zone. Therefore, the observed arrangement of pinwheel centers seems to be related to the orthogonality between iso-orientation contours and the area 17/18 transition zone, and it is speculated that these two properties might have a common origin, that is, a boundary effect. To clarify their relationship and possible underlying mechanisms, we conducted a simulation study.

Simulation Study

The details of the simulation method is described in Materials and Methods. Briefly, we used a modified bandpass filter model (Rojer and Schwartz, 1990) and Swindale's model (Swindale, 1982) to construct an orientation preference map. In these models, near-excitatory far-inhibitory lateral interaction is assumed (Rojer and Schwartz, 1990; Swindale, 1982). To realize the orthogonality between iso-orientation contours and the areal border, we introduced anisotropy in the lateral interaction (Swindale, 1980; Rojer and Schwartz, 1990) in three different ways: (A) only far-inhibitory interaction is elongated parallel to the border; (B) both near-excitatory and far-inhibitory interactions are elongated orthogonal to the border; and (C) only near-excitatory interaction is elongated orthogonal to the border. The shapes of these interactions are illustrated in the top part of Figure 5*A–C*. We conducted simulations 400 times for each of these interactions, by using the bandpass filter model. Some of the results are illustrated in the bottom part of Figure 5*A–C*. In all of them, the orthogonality was realized to a degree similar to the experimental results (Fig. 5*D*). However, in the case of (B), 95.2% of simulations resulted in no significant tendency in the distribution of pinwheel centers (Fig. 5*E*). Therefore, orthogonality does not necessarily lead to the systematic arrangement of pinwheel centers.

On the other hand, in the cases of (A) and (C), pinwheel centers of the same type tend to be aligned parallel to the areal border, in a way similar to that observed in our results. In 72.8 and 69.5% of simulations in the cases of (A) and (C) respectively, pinwheel pairs of the same type tend to be aligned parallel to the areal border. In 26.3 and 22.3% of simulations in the cases of (A) and (C), pinwheel pairs of opposite types also tend to be located orthogonal to the border. These results suggest that what is important for the systematic arrangement of pinwheel centers is difference in the shapes of near-excitatory and far-inhibitory interactions (that is, $\sigma_{Ey}/\sigma_{Ex} > \sigma_{Iy}/\sigma_{Ix}$). If such a difference exists, both orthogonality and the systematic arrangement of pinwheel centers will emerge. As neural correlates, two possibilities can be considered corresponding to (A) and (C): (i) truncation of the lateral inhibitory interaction at the areal border, as suggested by Swindale (1980); and (ii) elongation of lateral excitatory interaction orthogonal to the border. These possibilities cannot be discriminated from this study and further anatomical and physiological studies are required.

In the cases of (A) and (C), while pinwheel pairs of the same type tend to be aligned in a row parallel to the border, the alignment often appears in a single row, and alternating rows of pinwheel centers according to their types were observed

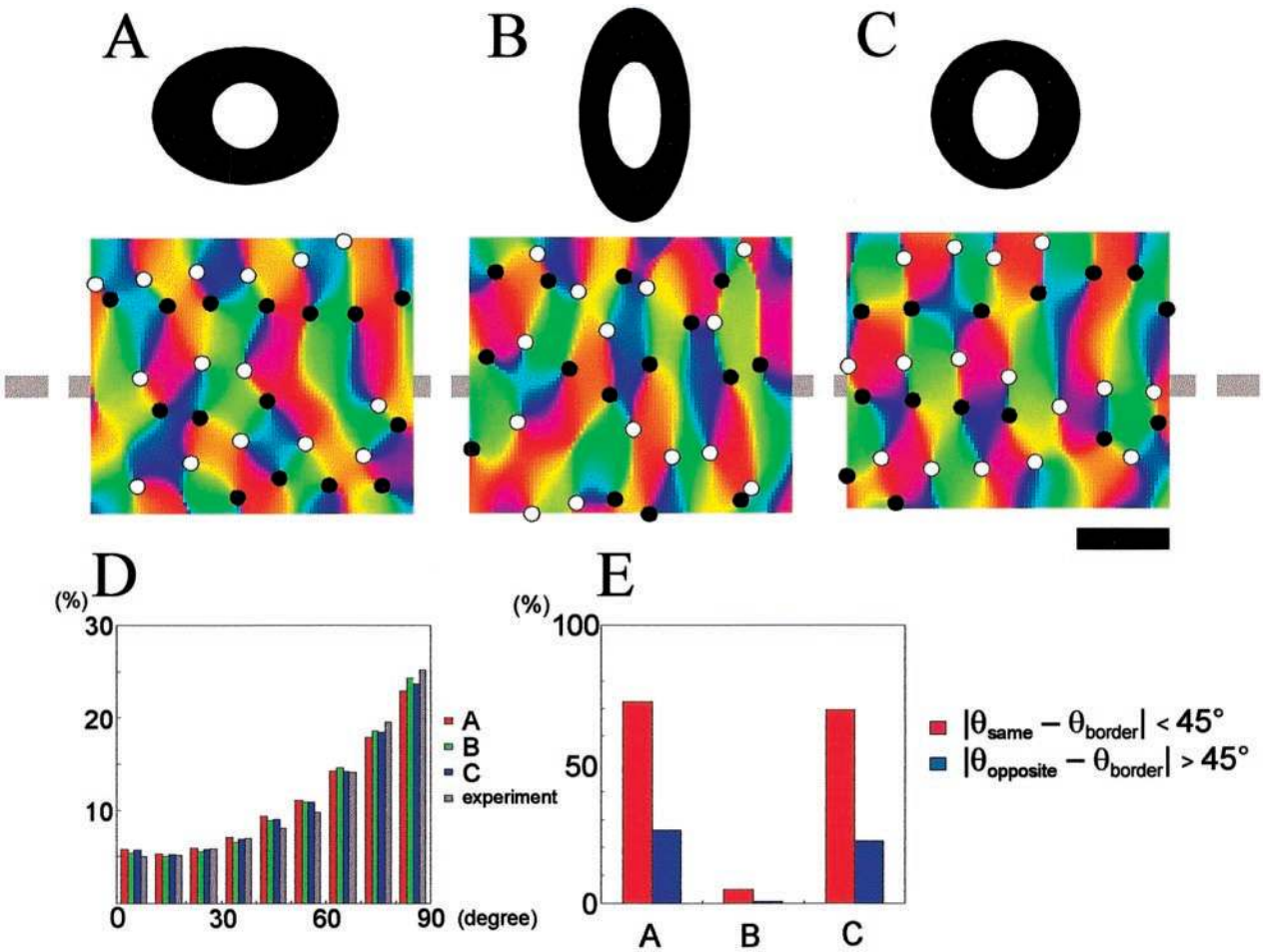

Figure 5. Simulation results. (*A–C*) Top: shapes of near-excitatory far-inhibitory lateral interaction kernels. The central white region shows excitatory interaction and the surround black region shows inhibitory interaction. Anisotropy in (*A*) and (*B*) is overemphasized for ease to see. Bottom: examples of simulation results obtained from three different types of interactions. The angle of the preferred orientation in each pixel is coded by the hue of the color. Black spots represent clockwise pinwheel centers and white spots represent counterclockwise pinwheel centers. A gray dashed line in the background shows direction of the areal border. Scale bar: 1 mm. (*D*) Histograms of relative angles between the iso-orientation contours and the direction of the areal border, obtained in the same manner as in Figure 4*B*. Each histogram for A, B or C was obtained from average of 400 simulations with the shape of interaction of (A), (B) or (C), respectively. The histogram for 'experiment' indicates the experimental results within the transition zone. (*E*) Percentage of simulations (in $n = 400$) which indicated statistically significant arrangement of pinwheel centers of the same type or opposite types. The statistical significance of the arrangement was evaluated by $|\theta_{same} - \theta_{border}| < 45°$ ($P < 0.05$) for pinwheel pairs of the same type and by $|\theta_{opposite} - \theta_{border}| > 45°$ ($P < 0.05$) for pinwheel pairs of opposite types.

infrequently. This suggests that some additional condition has to be considered. In the experimental results, the axes of anisotropy were not totally identical for each iso-orientation domain. The differences of these axes were within a range of 20°. When we incorporated such difference in the axes of anisotropy in the cases of (A) and (C), alternating rows of pinwheel centers according to their types often emerged, and the statistical results were also greatly improved (pinwheel pairs of the same type tend to be aligned parallel to the border in 82.8% of simulations, while pinwheel pairs of opposite types tend to be aligned orthogonal to the border in 59.0% of simulations). We succeeded in reproducing all the results by using Swindale's model (Swindale 1982).

To summarize, our simulation study suggests that the orthogonality between iso-orientation contours and the area 17/18 transition zone does not necessarily lead to the systematic arrangement of pinwheel centers, and that both the orthogonality and the systematic arrangement are caused by the same mechanism.

In conclusion, we suggest that the area 17/18 transition zone imposes a profound restriction on the pattern formation of orientation preference maps: the areal border not only makes iso-orientation contours run orthogonal to the border, but also arranges the orientation pinwheel centers to form a unique geometric pattern.

Notes

K.O. is supported by a JSPS Research Fellowship for Young Scientists and thanks Professor Yasushi Miyashita for his continuous encouragement. We thank Tomoya Saito for his assistance in the data analyses and simulations, and Drs Kathleen S. Rockland and Raymond T. Kado for the very helpful comments on earlier version of the manuscript.

Address correspondence to Dr Shigeru Tanaka, Laboratory for Neural Modeling, Brain Science Institute, RIKEN, Wako-shi, Saitama 351-0198, Japan. Email: shigeru@postman.riken.go.jp.

References

Bartfeld E, Grinvald A (1992) Relationships between orientation-preference pinwheels, cytochrome oxidase blobs, and ocular-dominance columns in primate striate cortex. Proc Natl Acad Sci USA 89:11905–11909.

Blasdel GG (1992) Orientation selectivity, preference, and continuity in monkey striate cortex. J Neurosci 12:3139–3161.

Bonhoeffer T, Grinvald A (1991) Iso-orientation domains in cat visual cortex are arranged in pinwheel-like patterns. Nature 353:429–431.
Bonhoeffer T, Grinvald A (1996) Optical imaging based on intrinsic signals: the methodology. In: Brain mapping: the methods (Toga A, Mazziotta JC, eds), pp. 55–97. San Diego, CA: Academic.
Bonhoeffer T, Kim DS, Malonek D, Shoham D, Grinvald A (1995) Optical imaging of the layout of functional domains in area 17 and across area 17/18 border in cat visual cortex. Eur J Neurosci 7:1973–1988.
Bosking WH, Zhang Y, Schofield B, Fitzpatrick D (1997) Orientation selectivity and the arrangement of horizontal connections in tree shrew striate cortex. J Neurosci 17:2112–2127.
Braitenberg V, Braitenberg C (1979) Geometry of orientation columns in the visual cortex. Biol Cybern 33:179–186.
Chapman B, Stryker MP, Bonhoeffer T (1996) Development of orientation preference maps in ferret primary visual cortex. J Neurosci 16: 6443–6453.
Crair MC, Ruthazer ES, Gillespie DC, Stryker MP (1997a) Ocular dominance peaks at pinwheel center singularities of the orientation map in cat visual cortex. J Neurophysiol 77:3381–3385.
Crair MC, Ruthazer ES, Gillespie DC, Stryker MP (1997b) Relationship between the ocular dominance and orientation maps in visual cortex of monocularly deprived cats. Neuron 19:307–318.
Crair MC, Gillespie DC, Stryker MP (1998) The role of visual experience in the development of columns in cat visual cortex. Science 279: 566–570.
Das A, Gilbert CD (1997) Distortions of visuotopic map match orientation singularities in primary visual cortex. Nature 387:594–598.
Diao YC, Jia WG, Swindale NV, Cynader MS (1990) Functional organization of the cortical 17/18 border region in the cat. Exp Brain Res 79:271–282.
Erwin E, Obermayer K, Schulten K (1995) Models of orientation and ocular dominance columns in the visual cortex: a critical comparison. Neural Computat 7:425–468.
Gotz KG (1988) Cortical templates for the self-organization of orientation specific d- and l-hypercolumns in monkeys and cats. Biol Cybern 58:213–223.
Greenside HS, Coughran WM Jr, Schryer NL (1982) Nonlinear pattern formation near the onset of Rayleigh–Benard convection. Phys Rev Lett 49:726–729.
Hubel DH, Wiesel TN (1962) Receptive fields, binocular interaction and functional architecture in the cat's visual cortex. J Physiol 160: 106–154.
Hubel DH, Wiesel TN (1963) Shape and arrangement of columns in cat's striate cortex. J Physiol 165:559–568.
Hubel DH, Wiesel TN, LeVay S (1977) Plasticity of ocular dominance columns in the monkey striate cortex. Phil Trans R Soc (Lond) B 278:377–409.
Hubener M, Shoham D, Grinvald A, Bonhoeffer T (1997) Spatial relationship among three columnar systems in cat area 17. J Neurosci 17:9270–9284.
Humphrey AL, Skeen LC, Norton TT (1980) Topographic organization of the orientation column system in the striate cortex of the tree shrew (*Tupaia glis*). II. Deoxyglucose mapping. J Comp Neurol 192: 544–566.
Law MI, Zahs KL, Stryker MP (1988) Organization of primary visual cortex (area 17) in the ferret. J Comp Neurol 278:157–180.
LeVay S, Hubel DH, Wiesel TN (1975) The pattern of ocular dominance columns in macaque visual cortex revealed by a reduced silver stain. J Comp Neurol 159:559–576.
Linsker R (1986) From basic network principles to neural architecture: emergence of orientation columns. Proc Natl Acad Sci USA 83: 8779–8783.
Livingstone MS, Hubel DH (1982) Thalamic inputs to cytochrome oxidase-rich regions in monkey visual cortex. Proc Natl Acad Sci USA 79:6098–6101.
Lowel S, Singer W (1987) The pattern of ocular dominance columns in flat-mounts of the cat visual cortex. Exp Brain Res 68:661–666.
Lowel S, Singer W (1990) Tangential intracortical pathways and the development of iso-orientation bands in cat striate cortex. Dev Brain Res 56:99–116.
Lowel S, Freeman B, Singer W (1987) Topographic organization of the orientation column system in large flat-mounts of the cat visual cortex: a 2-deoxyglucose study. J Comp Neurol 255:401–415.
Miller KD (1994) A model for the development of simple cell receptive fields and the ordered arrangement of orientation columns through activity-dependent competition between ON- and OFF-center inputs. J Neurosci 14:409–441.
Movshon JA, Thompson ID, Tolhurst DJ (1978) Spatial and temporal contrast sensitivity of neurons in areas 17 and 18 of the cat's visual cortex. J Physiol 283:101–120.
Obermayer K, Blasdel GG (1993) Geometry of orientation and ocular dominance columns in monkey striate cortex. J Neurosci 13: 4114–4129.
Obermayer K, Blasdel GG (1997) Singularities in primate orientation maps. Neural Computat 9:555–575.
Olavarria JF (1996) Non-mirror-symmetric patterns of callosal linkages in areas 17 and 18 in cat visual cortex. J Comp Neurol 366:643–655.
Orban GA, Kennedy H, Maes H (1980) Functional changes across the 17–18 border in the cat. Exp Brain Res 39:177–186.
Otsuka R, Hassler R (1962) Uber aufbau und gliderung der corticalen sehsphare bei der katze. Arch Psychiatr Z Ges Neurol 203:212–234.
Payne BR (1990) Representation of the ipsilateral visual field in the transition zone between areas 17 and 18 of the cat's visual cortex. Vis Neurosci 4:445–474.
Payne BR (1991) Visual-field map in the transcallosal sending zone of area 17 in the cat. Vis Neurosci 7:201–219.
Payne BR, Siwek DF (1991) Visual-field map in the callosal recipient zone at border between areas 17 and 18 in the cat. Vis Neurosci 7:221–236.
Ratzlaff EH, Grinvald A (1991) A tandem-lens epifluorescence macroscope: hundred-fold brightness advantage for wide-field imaging. J Neurosci Methods 36:127–137.
Rojer AS, Schwartz EL (1990) Cat and monkey cortical columnar patterns modeled by bandpass-filtered 2D white noise. Biol Cybernet 62:381–391.
Sengpiel F, Stawinski P, Bonhoeffer T (1999) Influence of experience on orientation maps in cat visual cortex. Nature Neurosci 2:727–732.
Shatz CJ (1990) Impulse activity and the patterning of connections during CNS development. Neuron 5:745–756.
Sheth BR, Sharma J, Rao SC, Sur M (1996) Orientation maps of subjective contours in visual cortex. Science 274:2110–2115.
Stryker MP, Harris W (1986) Binocular impulse blockade prevents the formation of ocular dominance columns in cat visual cortex. J Neurosci 6:2117–2133.
Stryker MP, Strickland SL (1984) Physiological segregation of ocular dominance columns depends on the pattern of afferent electrical activity. Invest Ophthalmol Vis Sci (suppl) 25:278.
Swindale NV (1980) A model for the formation of ocular dominance stripes. Proc R Soc Lond B 208:243–64.
Swindale NV (1982) A model for the formation of orientation columns. Proc R Soc Lond B 215:211–230.
Swindale NV, Matsubara JA, Cynader MS (1987) Surface organization of orientation and direction selectivity in cat area 18. J Neurosci 7: 1414–1427.
Tal D, Schwartz EL (1997) Topological singularities in cortical orientation maps: the sign theorem correctly predicts orientation column patterns in primate striate cortex. Network 8:229–238.
Tanaka S (1990) Theory of self-organization of cortical maps: mathematical framework. Neural Networks 3:625–40.
Tootell RBH, Silverman MS, DeValois RL, Jacobs GH (1983) Functional organization of the second cortical visual area in primates. Science 220:737–739.
Tusa RJ, Palmer LA, Rosenquist AC (1978) The retinotopic organization of area 17 (striate cortex) in the cat. J Comp Neurol 177:213–236.
Weliky M, Katz LC (1997) Disruption of orientation tuning in visual cortex by artificially correlated neuronal activity. Nature 386: 680–685.
Wiesel TN, Hubel DH (1965) Comparison of the effects of unilateral and bilateral eye closure on cortical unit responses in kittens. J Neurophysiol 28:1029–1040.
Wolf F, Bauer HU, Pawelzik K, Geisel T (1996) Organization of the visual cortex. Nature 382, 306.